



## RESEARCH ARTICLE

# Tissue Recognition Based on Electrical Impedance Classified by Support Vector Machine in Spinal Operation Area

Bingrong Chen, MM<sup>1</sup>, Yongwang Shi, BS<sup>2</sup>, Jiahao Li, MM<sup>1</sup>, Jiliang Zhai, MD<sup>1</sup> , Liang Liu, PhD<sup>3</sup>, Wenyong Liu, PhD<sup>4</sup>, Lei Hu, PhD<sup>5</sup>, Yu Zhao, MD<sup>1</sup> 

<sup>1</sup>Department of Orthopaedic Surgery, Peking Union Medical College Hospital, Chinese Academy of Medical Sciences and Peking Union Medical College, <sup>2</sup>MD Program, Chinese Academy of Medical Sciences & Peking Union Medical College, <sup>3</sup>China Astronaut Research and Training Center and School of <sup>4</sup>Biological Science and Medical Engineering and <sup>5</sup>Mechanical Engineering and Automation, Beihang University, Beijing, China

**Objective:** One of the major difficulties in spinal surgery is the injury of important tissues caused by tissue misclassification, which is the source of surgical complications. Accurate recognition of the tissues is the key to increase safety and effect as well as to reduce the complications of spinal surgery. The study aimed at tissue recognition in the spinal operation area based on electrical impedance and the boundaries of electrical impedance between cortical bone, cancellous bone, spinal cord, muscle, and nucleus pulposus.

**Methods:** Two female white swines with body weight of 40 kg were used to expose cortical bone, cancellous bone, spinal cord, muscle, and nucleus pulposus under general anesthesia and aseptic conditions. The electrical impedance of these tissues at 12 frequencies (in the range of 10–100 kHz) was measured by electrochemical analyzer with a specially designed probe, at 22.0–25.0°C and 50%–60% humidity. Two types of tissue recognition models - one combines principal component analysis (PCA) and support vector machine (SVM) and the other combines SVM and ensemble learning - were constructed, and the boundaries of electrical impedance of the five tissues at 12 frequencies of current were figured out. Linear correlation, two-way ANOVA, and paired *T*-test were conducted to analyze the relationship between the electrical impedance of different tissues at different frequencies.

**Results:** The results suggest that the differences of electrical impedance mainly came from tissue type ( $p < 0.0001$ ), the electrical impedance of five kinds of tissue was statistically different from each other ( $p < 0.0001$ ). The tissue recognition accuracy of the algorithm based on principal component analysis and support vector machine ranged from 83%–100%, and the overall accuracy was 95.83%. The classification accuracy of the algorithm based on support vector machine and ensemble learning was 100%, and the boundaries of electrical impedance of five tissues at various frequencies were calculated.

**Conclusion:** The electrical impedance of cortical bone, cancellous bone, spinal cord, muscle, and nucleus pulposus had significant differences in 10–100 kHz frequency. The application of support vector machine realized the accurate tissue recognition in the spinal operation area based on electrical impedance, which is expected to be translated and applied to tissue recognition during spinal surgery.

**Address for correspondence** Lei Hu, PhD, Beihang university, School of Mechanical Engineering and Automation, No. 37, Xueyuan Road, Haidian District, Beijing 100191, China Tel: +8613311269371; Fax: 01082317850; Email: [hulei9971@sina.com](mailto:hulei9971@sina.com); Yu Zhao, MD, Department of Orthopaedics, Peking Union Medical College Hospital, Chinese Academy of Medical Sciences and Peking Union Medical College, Dongcheng District Shuaifuyuan No.1, Beijing 100730, China, Tel: +8615601089898; Fax: 01069152809; Email: [zhaoyupumch@163.com](mailto:zhaoyupumch@163.com).

Grant sources: This work was supported by the Ministry of Science and Technology, China (grant number: 2018YFB1307603) and the Natural Science Foundation of Beijing Municipality, China (grant number: L192061).

Disclosure: There is not any financial support or relationships that may pose conflict of interest.

Received 25 March 2022; accepted 25 June 2022



**Key words:** Bioelectrical impedance; Ensemble learning; Principal component analysis; Support vector machine; Tissue recognition

## Introduction

There are various important structures in the operation area of spine surgery including the spinal cord, nerve roots, and blood vessels. Accurate recognition of these tissues is a challenge for surgeons. Inaccurate judgment of spinal tissue may lead to incorrect operation, resulting in nerve and vascular injuries<sup>1</sup>. It is a hot research topic to find an objective and accurate method for tissue identification in the spinal surgery area<sup>2</sup>. In addition to traditional imaging methods, tissue recognition techniques based on physical information such as force, acoustics, and bioelectrical impedance are also widely studied<sup>3-8</sup>.

Bioelectrical impedance is a kind of electrical characteristics of biological tissues, based on which are there tissue type identification methods that are considered to be simple in measurement, sensitive, and real-time<sup>9</sup>. Bioelectrical impedance measures tissue-specific characteristics by measuring the impedance of an equivalent circuit consisting of intracellular fluid (resistance), extracellular fluid (resistance), and cell membrane (capacitance)<sup>10</sup> (Figure 1). The impedance information of tissues can be obtained by designing probes according to the characteristics of tissues<sup>11</sup>. Bioelectrical impedance can achieve differentiated recognition in both bone and soft tissues, while imaging, force, and acoustics-based recognition methods have is good for bone, but poor for soft tissues<sup>2,12</sup>. Although the previous studies have confirmed differences in the electrical impedance of tissues at the spinal surgery site, none of them have reported the boundaries for the impedance classification of different tissues at the spinal surgery site.

Support Vector Machine (SVM) is a commonly used machine learning algorithm, which is good on classification tasks and performs well in many medical classification problems<sup>13</sup>. It can provide boundaries whose distance to the samples are maximized data boundary in high dimensional feature space<sup>14</sup>. The excellent generalization ability and intuitive classification results of SVM have attracted the attention of researchers<sup>15,16</sup>. It may be helpful to the classification of tissue electrical impedance in the spinal surgery area. Electrical impedance is usually measured at multiple frequencies at the same time, and the data dimension is high. In order to improve the accuracy and generalization ability of the model, it is usually appropriate to reduce the dimension of the data.

Principal component analysis (PCA) is a basic dimension reduction method in machine learning, which transforms high-dimensional data into features of low-dimensional space<sup>17</sup>. For data with a high dimensional, more accurate results can be obtained by performing PCA before classification or regression<sup>18,19</sup>. Ensemble learning is a classifier combination paradigm, which can gather the classification results of multiple classifiers by voting to get better classification performance and stronger generalization ability<sup>20,21</sup>. The performance of SVM can be improved by combining multiple SVM classifiers with ensemble learning<sup>22</sup>.

The objectives of this study were as follows: (i) electrical impedance data were collected from different tissues at the spinal operation area *in vivo*; (ii) SVM, combined with PCA or ensemble learning, were used to classify and to find the boundaries of electrical impedance of different tissues in spinal operation area; (iii) the accuracy of classification was verified through animal experiments.

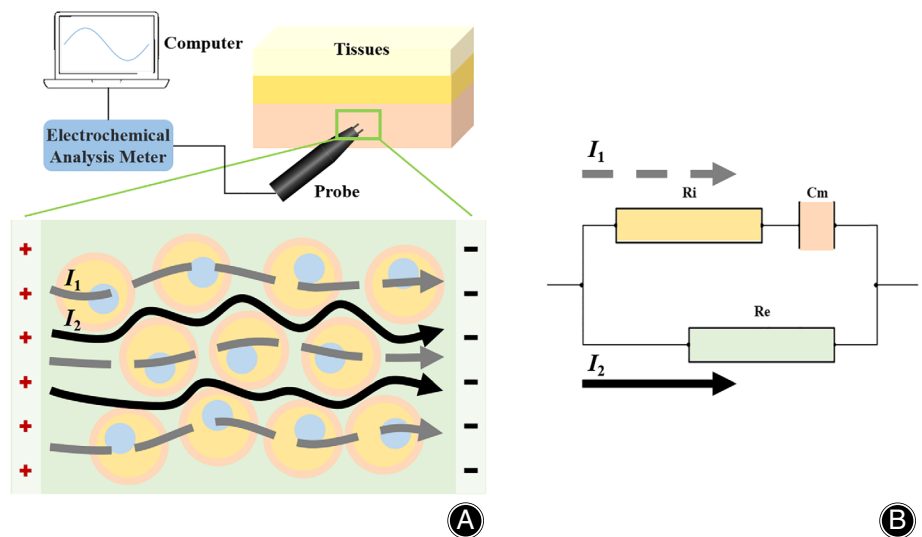


**Fig. 1** Schematic diagram of electrical impedance measurement. (A) Schematic diagram of cell and extracellular fluid currents; (B) Bioelectrical impedance equivalent circuit model:  $R_i$  intracellular fluid resistance,  $R_e$  extracellular fluid resistance,  $C_m$  membrane capacitance; Gray dotted line: intracellular fluid current, black solid line: extracellular fluid current

## Materials and Methods

### Experimental Objects

Two female British white swines, weighing about 40 kg (provided by Beijing Fulong Tengfei Experimental Animal Research Institute Co., LTD.). In this study, the impedance of five types of spinal tissues were measured: cortical bone, cancellous bone, muscle, spinal cord, and nucleus pulposus, all of which were measured before the swines were executed.

### Electrical Impedance Acquisition Platform

The electrical impedance acquisition platform applied in this study consists of an electrochemical analyzer, a computer, an electrical impedance acquisition system, and a probe (Figure 2A). The electrochemical analyzer is CHI604E (CH Instruments Ins. Austin, TX, USA). The electrical impedance measurement system is the electrical impedance acquisition module of Model 600E Series Workstation (CH Instruments Ins. Austin, TX, USA), which is loaded on Windows 10 system computer and connected with the electrochemical analyzer through USB. In this study, a parallel two-electrode electrical impedance probe was independently designed according to the characteristics of the spinal surgery area, which was connected to the electrochemical analyzer through electrode wires (Figure 2B).

### Tissue Exposure at the Spinal Operation Area

In this study, cortical bone, cancellous bone, muscle, spinal cord, and nucleus pulposus of experimental swines were exposed by posterior spinal surgery. The swines were fasted for 24 h before surgery and anesthetized by intravenous infusion of pentobarbital sodium. After anesthesia induction, the swines were placed in prone position and anesthetized by inhalation of isoflurane. The vital signs of the swines were monitored during surgery. The skin, after disinfection, draping, midline incision along the back skin incision, stripping

step by step by the subcutaneous tissue, vertebral muscles and other soft tissue, vertebrae, nucleus pulposus, such as structure, with periosteum stripping device eliminating spines and connective tissue, show of cortical bone, vertebral plate surface with rongeur bite in addition to the part of the spine to show cancellous bone, remove vertebral plate to expose the spinal cord.

### Electrical Impedance Data Acquisition

As the value of bioelectrical impedance is greatly affected by environmental conditions, this study is controlled in a constant temperature (temperature: 22.0–25.0 °C) and constant humidity (humidity: 50%–60%) environment to reduce the interference of environmental factors. Connect the electrical impedance acquisition platform, then use the standard resistance of 1000  $\omega$  for system correction, and set the initial level to 0.5 V. Each set of data includes the impedance at 12 frequencies: 10010 Hz, 12210 Hz, 14650 Hz, 17820 Hz, 21480 Hz, 26120 Hz, 31740 Hz, 38330 Hz, 46390 Hz, 56150 Hz, 68120 Hz, 82520 Hz. We designed a bipolar probe consisting of two needle-like electrodes with fixed distances to achieve compact contact with various tissues, to ensure accurate acquisition of electrical impedance (Figure 1A). Tissues were fully exposed before detection. The probe was placed on the surface of the spinous process to collect the cortical bone electrical impedance, placed on the bone tinside the spinous process to collect the spongy bone electrical impedance, placed on the paraspinal muscle to measure the muscle electrical impedance, placed on the spinal nerve to collect the spinal cord electrical impedance, and placed on the tissue between the upper and lower vertebral bodies to collect the myeloid nuclear impedance (Figure 2C). The mean value of electrical impedance measured by three researchers on the same part was taken as the single impedance measurement value. Between the two measurements, tissues on the surface of the electrode head were wiped with normal saline and



**Fig. 2** Electrical impedance acquisition platform and experimental process. (A) Electrical impedance acquisition platform and experimental environment; (B) Electrical impedance measurement probe; (C) Electrical impedance measurement process. The picture shows the electrical impedance measurement process of cortical bone on the spinous process

clean gauze to ensure that the electrode head was clean and dry. Electrical impedance values of 12 frequencies of each tissue are measured and stored in txt. format. Each tissue shall ensure at least three groups of valid data. Data collected from two experimental swines were used as training set and test set, respectively.

### Data Pre-Processing

The electrical impedance data of five kinds of tissues at 12 frequencies were imported into Excel (version 2019, Microsoft, Redmond, WA, USA). One person was responsible for importing and the other person was responsible for checking to ensure the data was valid and accurate. As electrical impedance is susceptible to animal breathing fluctuation and hand shaking in the process of collection, we eliminated some data groups, and the elimination criteria are as follows: (1) coefficient of variation within the group  $>0.15$ ; (2) The mean difference between one data set in the group and other data set at the same tissue at the same frequency is more than three times the standard deviation; (3) There were values less than  $Q1-1.5iQR$  or greater than  $Q3+1.5iQR$  in the group.

### Statistics

SPSS 26.0 (IBM, Armonk, New York, USA) software was used for statistical analysis of the preprocessed experimental data. All tests were conducted by two-sided test,  $p < 0.05$  was considered statistically significant, and  $p < 0.01$  was considered extremely significant. The electrical impedance data were described according to tissue type and frequency, and the correlation between impedance and frequency was analyzed by correlation. Two-way ANVOA was used to analyze the effect of tissue type and frequency on the difference of electrical impedance values. The electrical impedance difference of different tissues was verified by paired T test (same frequency paired).

### Classification Based on SVM and PCA

For each tissue, the impedance at 12 frequencies was collected; thus, each sample is represented by a 12-dimensional vector. To avoid over-fitting caused by the high complexity of the model, a simple model with the input being low-dimensional is appropriate. Therefore, PCA is used to reduce the dimensionality of the input from 12 to 2, as the two largest principal components of feature vectors of the training set already accounts for 99.85% of the variance of features of training samples. PCA is trained on the training set, and then applied to the feature vectors of training samples and test samples. The implementation of PCA is decomposition. PCA from scikit-learn (version 1.0.2) on Python (version 3.7.3) with all parameters being default except the target dimensionality being 2.

After dimension reduction, linear SVM is used for classification, since the transformed feature vectors are nearly linear separable. The implementation is svm. SVC from scikit-learn on Python, with the versions as above. The parameters are set as default expect the normalization coefficient being 100. SVM is trained on the training set, and then tested on the test set. In both training and testing, the accuracy of the classification is used to evaluate the model performance.

### Classification Based on SVM and Ensemble Learning

In the previous subsection, PCA is adopted to reduce the complexity of the model. Ensemble learning is also adopted to achieve this. For each frequency, a simple one-dimensional SVM can be built with the input being the impedance at that frequency; in total, 12 SVMs can be built, each labeled by C\_1 to C\_12, with C\_1 corresponding to the lowest frequency and C\_12 the highest. The implementation of SVM is as above. Similar to Random Forest, these base models are of high diversity since each uses a different feature as input. The diversity accounts for the better performance of the ensemble model in Random Forest; therefore, it is speculated that the ensemble model of the 12 SVMs is better than any of the base model.

**TABLE 1** Electrical impedance of the first experiment

Frequency/Hz	Cortical Bone		Cancellous Bone		Spinal Cord		Muscle		Nucleus Pulposus	
	Mean/ $\Omega$	SD	Mean/ $\Omega$	SD	Mean/ $\Omega$	SD	Mean/ $\Omega$	SD	Mean/ $\Omega$	SD
10,010	82360.00	9013.92	8804.33	153.58	3597.00	388.47	767.86	85.42	339.73	6.62
12,210	81587.50	8861.66	8761.67	168.57	3522.67	420.36	755.22	78.82	328.47	6.60
14,650	80970.00	9008.41	8703.67	173.25	3480.83	440.30	739.44	82.28	319.18	6.19
17,820	80435.00	8655.62	8660.67	195.82	3418.67	486.49	725.36	75.51	310.70	6.46
21,480	79557.50	8487.18	8619.67	211.90	3347.67	556.06	714.98	74.91	304.67	6.46
26,120	78557.50	8065.52	8559.67	212.39	3314.00	556.79	703.96	73.18	297.87	6.98
31,740	77527.50	7766.51	8500.00	213.91	3285.17	542.11	696.40	73.63	292.50	7.46
38,330	76275.00	7539.15	8446.33	216.80	3245.50	544.62	686.72	74.71	289.60	7.41
46,390	74600.00	6902.20	8374.00	226.92	3205.33	530.52	680.08	75.09	286.43	7.46
56,150	72647.50	6615.44	8298.00	214.75	3167.50	549.21	672.80	70.40	283.73	7.28
68,120	69950.00	5875.91	8210.67	249.65	3134.83	541.16	665.54	64.25	281.55	6.90
82,520	66825.00	5131.41	8114.00	250.41	3112.67	532.88	659.16	61.93	280.05	6.58



Based purely on the performance on the training set, several best base models are chosen to be combined. For the ensemble model, it collects the predictions of each base model chosen, and one of the most frequently predicted classes is adopted as the output of the ensemble model. The ensemble model is then tested on the test set.

## Result

### Electrical Impedance of Five Tissues in Spinal Operation Area

The descriptive statistical results showed that the electrical impedance values of the tissues in the five spinal surgery

**TABLE 2** Electrical impedance of the second experiment

Frequency/Hz	Cortical Bone		Cancellous Bone		Spinal Cord		Muscle		Nucleus Pulposus	
	Mean/ $\Omega$	SD	Mean/ $\Omega$	SD	Mean/ $\Omega$	SD	Mean/ $\Omega$	SD	Mean/ $\Omega$	SD
10,010	22750.00	6558.19	10089.75	775.65	1337.00	84.67	631.58	93.73	351.18	21.51
12,210	21520.00	7538.32	10300.50	436.11	1339.00	97.73	650.58	105.39	355.06	22.77
14,650	23362.00	6702.50	10599.50	555.63	1354.60	104.02	672.52	118.21	360.20	23.26
17,820	22112.00	7295.98	10897.50	480.93	1355.60	94.77	693.04	134.15	363.30	21.58
21,480	21988.00	8008.96	10612.50	289.53	1364.60	106.42	710.54	132.11	368.48	22.80
26,120	22776.00	9614.50	9933.75	1449.94	1423.80	164.62	734.90	148.89	375.12	28.22
31,740	21904.00	8907.74	11232.50	489.79	1352.00	92.74	751.68	138.13	382.32	24.41
38,330	21296.00	7377.48	11425.00	793.66	1376.40	88.92	768.12	168.49	389.76	23.18
46,390	21318.00	8233.51	11225.00	438.82	1386.40	101.17	777.30	173.15	398.46	23.46
56,150	21092.00	8996.44	12237.50	440.10	1395.20	110.57	808.92	162.17	410.34	24.24
68,120	24158.00	9913.21	10256.75	1925.67	1409.20	89.48	897.02	197.58	420.94	20.61
82,520	20384.00	7519.51	12257.50	1086.20	1407.00	116.64	865.84	194.86	441.32	23.43

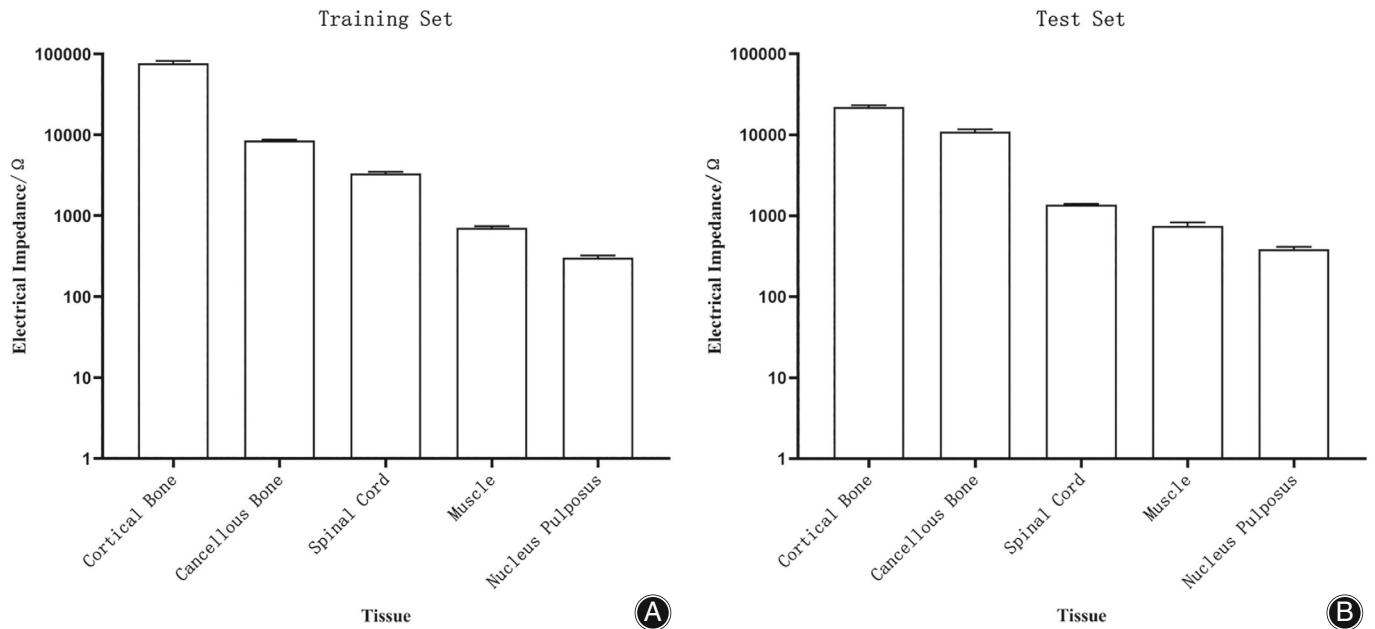


**Fig. 3** Impedance values of different tissues in two experiments. (A) Electrical impedance values of different tissues in the first experiment (training set collection process); (B) Electrical impedance values of different tissues in the second experiment (test set collection process). The vertical axis is logarithmic, with significant differences among tissues ( $p < 0.0001$ ).

**TABLE 3** The correlation between electrical impedance and frequency of experiment current

	Cortical Bone	Cancellous Bone	Spinal cord	Muscle	Nucleus Pulposus
Correlation	Negative	Negative	Negative	Negative	Negative
$p$ value	0.4841	0.0714	0.3460	<0.0001	<0.0001
Significance	non	non	non	***	***

areas measured at 12 frequencies in the two live animal experiments presented a pattern of cortical bone > cancellous bone > spinal cord > muscle > nucleus pulposus (Tables 1 and 2, Figure 3). Correlation analysis results showed that the electrical impedance of the five tissues was negatively correlated with the frequency range, that is, the electrical impedance decreased with the increase of measured frequency. The correlation between cortical bone, cancellous bone, and spinal cord was not significant, but that between muscle and nucleus pulposus was significant (Table 3, Figure 4). Two-factor ANOVA of repeated samples showed that the differences in electrical impedance values measured in this study were mainly related to tissue type and almost unrelated to measurement frequency (Table 4). Paired *T*-test was performed on the electrical impedance of the five tissues in the spinal surgery area based on frequency pairing, and the results showed that the electrical impedance of the five tissues was significantly different within the measured frequency range ( $p < 0.0001$ , Table 5).

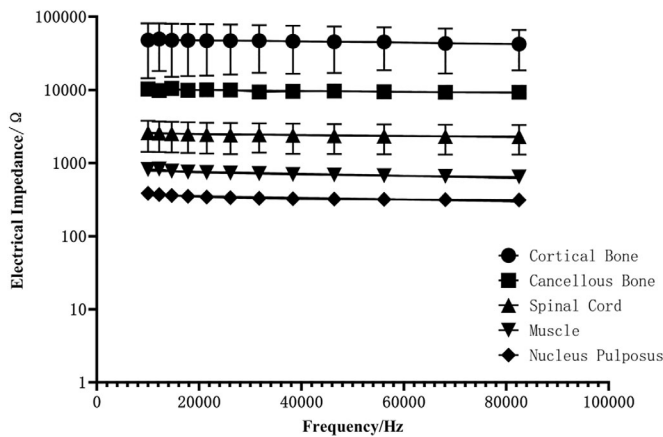


Fig. 4 The impedance of each tissue varies with frequency

**Result of Classification Based on SVM and PCA**

PCA showed the largest and the second largest principal component accounts for 99.54% and 0.31% of the variance of the features of the training samples; thus, the information of the original features were preserved by dimension reduction. The accuracy of the SVM using the two largest principal components was 100% on the training set and 95.83% on the test set (Table 5a); the regions of each class was shown in Figure 5A. Since the largest principal component accounts for 99.54% of the variance, this work also built a similar model using only the largest principal component: the accuracy was the same (Table 5b) while the regions of each class were simpler (Figure 5B).

**Result Based on SVM and Ensemble Learning**

This work built 12 one-dimensional SVMs (C<sub>1</sub>-C<sub>12</sub>), each accepted input of the impedance of the sample at a particular frequency. The boundaries (thresholds) of the impedance of various tissues at all frequencies were calculated (Table 6). The accuracy of these one-dimensional SVMs varied: 81–100% on the training set and 88–100% on the test set. Best ones are C<sub>1</sub>-C<sub>7</sub>: accuracy is 100% on both sets. This work, therefore, built an ensemble model on C<sub>1</sub>-C<sub>7</sub>, which achieve 100% accuracy on the training set and the test set.

**Discussion**

This study is the first to use machine learning combined with bioelectrical impedance method to identify and classify the electrical impedance of tissues in spinal surgery area, and it is the first to propose the bioelectrical impedance classification threshold of cortical bone, cancellous bone, spinal cord, muscle, and nucleus pulposus in spinal surgery area. In this study, it was found that the electrical impedance of cortical bone, cancellous bone, spinal cord, muscle, and nucleus pulposus in the spinal surgery area was significantly different within the measurement frequency of 10 kHz–100

TABLE 4 Results of two-way ANOVA with repeated samples					
Source	SS (Type III)	DF	MS	F value	p value
Tissue * Frequency	326,918,653	44	7,429,969	0.04347	$p > 0.9999$
Frequency	126,346,235	11	11,486,021	0.06720	$p > 0.9999$
Tissue	172,606,405,931	4	43,151,601,483	252.5	$p < 0.0001^{***}$
Residual	86,147,696,423	504	170,927,969		

TABLE 5 Result of classification based on PCA and SVM						
	Cortical Bone	Cancellous Bone	Spinal cord	Muscle	Nucleus Pulposus	Overall
a	100% (4/4)	100% (3/3)	83% (5/6)	100% (5/5)	100% (6/6)	96% (23/24)
b	100% (4/4)	100% (3/3)	83% (5/6)	100% (5/5)	100% (6/6)	96% (23/24)

a. the accuracy of classification of the SVM using the two largest principal components ; b. the accuracy of classification of the SVM using only the largest principal components.

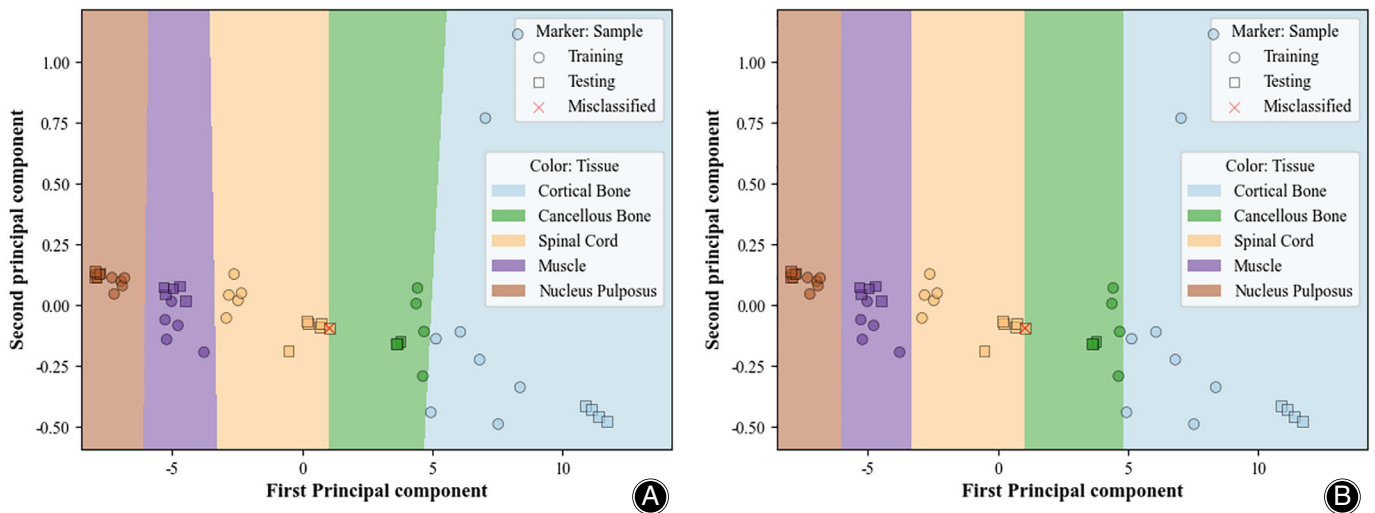


**Fig. 5** Result of classification based on PCA and SVM. (A) Result of classification of the SVM using the two largest principal components; (B) Result of classification of the SVM using only the largest principal components. The horizontal axis. The largest principal component. The vertical axis. The second largest principal component. ○. Training sample. □. Test sample. ×. Incorrectly classified sample.

**TABLE 6** The boundaries of impedance of five tissues in the area of spine surgery at 12 frequencies

Frequency	Cortical bone-Cancellous bone	Cancellous bone-Spinal cord	Spinal cord - Muscle	Muscle-Nucleus Pulposus
10,010	11524.30	4136.00	1237.19	584.95
12,210	10904.64	3583.53	1267.97	572.57
14,650	11713.14	4252.58	1184.20	548.63
17,820	11488.43	3958.88	1173.24	533.41
21,480	12199.85	3917.40	1157.43	519.55
26,120	11859.49	3917.38	1096.60	514.96
31,740	11968.93	3824.45	1127.67	508.32
38,330	11272.55	3925.71	1076.20	493.05
46,390	11449.98	3873.95	1061.60	477.57
56,150	12129.78	3851.27	1032.83	474.70
68,120	11482.76	3770.67	1002.94	462.12
82,520	12178.99	3590.27	977.46	453.70

kHz. The accuracy of PCA combined with SVM was 96%, while the accuracy of SVM combined with ensemble learning was 100%. By 100% identifying these tissues, we can achieve accurate identification of pedicle penetration.

Currently, spinal surgeons often use tactile feedback from ball-tipped probe to identify whether an open screw path has broken through the cortical bone with an accuracy of 62%–91%<sup>23</sup>, which is not sufficient for the safety of spine surgery. In clinical practice, improper manipulation of ball-tipped probe after pedicle penetration may cause mechanical damage to nerves. Study using electrical impedance for tissue classification had achieved 96% accuracy for pedicle penetration<sup>24</sup>. However, the accuracy of identifying pedicle screw penetration did not represent the accuracy of tissue classification. The accurate rate of this study was higher than both of them, and our method could realize more refined tissue classification. It was for the following reasons.

First of all, due to the high sensitivity<sup>25</sup>, the accuracy of electrical impedance in tissue classification was higher than the traditional tactile feedback. Secondly, as different probes were suitable for different operation scenarios<sup>11</sup>, we target designed a bipolar probe for the spinal surgery area, which ensure the accurate and robust data acquisition. Thirdly, we applied SVM and ensemble learning, which were good at classification<sup>13</sup>, to find the specific threshold and quantitatively analyze the obvious and potential difference of electrical impedance of different tissues, while the identification of tissues by ball-tipped probe and electrical impedance in previous studies were based on qualitative or statistical significance estimate. To sum up, electrical impedance classification, specific probe, and machine learning methods enabled us to achieve 100% tissue classification accurate rate, which can further avoid the pedicle penetration caused by tissue misclassification.

### **Electrical Impedance Difference of Tissues in Spinal Operation Area**

Studies have shown that there are statistical differences in electrical impedance of different tissues<sup>25–27</sup>. Studies have found that there are significant differences in the electrical impedance of muscle, ovary, testis, liver, kidney, and other tissues of cattle. Accurate identification of these tissues can be achieved according to the electrical impedance, which proves the high sensitivity of electrical impedance in tissue classification<sup>28</sup>. Other researchers have realized real-time identification of fat, muscle, blood, liver, spleen, and other tissues in live animal experiments based on significant differences in bioelectrical impedance between tissues<sup>29</sup>. The results of these studies have inspired us to use electrical impedance techniques for tissue classification in the spinal surgery area. In this study, an electrical impedance acquisition platform was also built, and an electrical impedance probe was designed for the spinal operation area of swines. The impedance values of cortical bone, cancellous bone, spinal cord, muscle, and intervertebral disc nucleus pulposus in living swines were collected. In addition, the higher the frequency of electrical impedance measurement, the more significant the current through the intracellular matrix<sup>9</sup>. Therefore, this study applied the frequency range of 10 kHz–100 kHz to collect the electrical impedance of different tissues. The results confirmed that the electrical impedance values of the five tissues in the spinal surgery area were statistically different, which could be used as the basis for tissue classification. Similar to the results of previous studies<sup>8,30,31</sup>, we found that the impedance value of bone tissue was higher than that of non-bone tissue, and the impedance value of the five spinal tissues in descending order were cortical bone, cancellous bone, spinal cord, muscle, and nucleus pulposus. We found that the electrical impedance of all five tissues decreased with the increase of measurement frequency. Among which, there were significant correlations between measurement frequency and impedance value in muscle and nucleus pulposus, which was consistent with the results of previous studies<sup>12</sup>. Considering both electricity and physiology, the distinction of impedance value may result from the difference of water content, free ion concentration in extracellular fluid between these tissues. The significant correlations between measurement frequency and impedance value may result from the membrane permeability and free ion concentration in intracellular fluid.

### **The Electrical Impedance of Spinal Tissue Classified by SVM**

Artificial intelligence algorithms have been widely used in a variety of medical scenarios, including image-based tissue recognition, bone recognition based on force signals, bone recognition based on sound signals, etc.<sup>6,32,33</sup>. According to the characteristics of physical information and the purpose of classification, different algorithms need to be applied. Previous studies have confirmed that the electrical impedance of spinal surgery area changes linearly with frequency<sup>34</sup>, and

the electrical impedance of different tissues varies significantly, with low complexity of data rules, which is suitable for classification by SVM. Some studies applied SVM algorithm to distinguish benign and malignant prostate tissue based on electrical impedance, with an accuracy of 81%<sup>35</sup>. Previous studies have found that the electrical impedance data measured in spinal surgery area are prone to interference and noise, and the electrical impedance data measured at multiple frequencies give a high dimension to the data set<sup>36</sup>. Support vector machine has good performance in low-complexity classification tasks, while principal component analysis can suppress noise to a certain extent and achieve data dimension reduction. Joint application can improve the generalization ability of classification methods<sup>37,38</sup>. At the same time, the classification of multiple tissues needs multiple classifiers. For the classification task with multiple classifiers, application ensemble learning can improve the accuracy of the classification task<sup>39–41</sup>. Considering the data rule complexity, model complexity, algorithm characteristics, and other factors comprehensively, this study uses the method of support vector machine to construct the classification model of five kinds of tissues and calculate the classification critical value of different tissues. The classification method of support vector machine combined with principal component analysis of our verification results has low accuracy in spinal cord identification and cannot meet clinical needs. Considering ensemble learning can fuse classifiers to improve the overall classification performance, this study further adopts support vector machine ensemble learning method to classify. Based on this algorithm, 48 tissue classification critical values of five tissues at 12 frequencies were obtained in this study. In the validation of test sets, it was found that this method has higher accuracy and can meet clinical requirements. These data indicate that support vector machines can be used to classify bioelectrical impedance in spinal surgery and provide reliable tissue identification information for spinal surgeons. This technique could be used to recognize tissues that are not easily discernible to the naked eye, during tissue dissection, decompression in open surgery. For example, we could use this technique to identify whether the lamina is penetrated, whether the spinal cord is injured during laminectomy, so as to avoid spinal cord injury. Furthermore, it can be extended to be utilized in minimally invasive spine and joint surgery.

### **Strength and Limitations**

In this study, the tissue recognition accuracy had achieved 100% in live animal experiments, which had not been achieved in similar studies. And we quantitatively obtained the classified electrical impedance threshold of the spine surgery field tissues for the first time. These exciting results are due to our first application of SVM, PCA, and ensemble learning to establish a method for spine surgical area tissue classification based on electrical impedance.

However, there are still some limitations to our study. Firstly, there was mis-classification between spinal cord and



cancellous bone based on PCA with SVM, due to the data set used in being small. This caused the mis-classification between spinal cord and cancellous bone based on PCA with SVM, so a larger data set is needed to train the algorithm with better performance of tissue recognition by PCA and SVM. Secondly, the interference of blood and flushing fluid in the surgical area was not completely removed in the measurement of tissue electrical impedance in this study, which may lead to deviation of results. Regardless of these limitations, this study provides a new idea for surgical area tissue recognition based on machine learning.

### Future Work

This technique could translate into a novel tissue classification probe. To translate this technique, the electrical impedance acquisition platform needs to be iteratively optimized. Clinical trials were conducted to establish human tissue electrical impedance data sets, and to further confirm the safety, effectiveness, reliability, and availability of the technique.

### Conclusion

In this study, the bioelectrical impedance of cortical bone, cancellous bone, spinal cord, muscle, and nucleus pulposus in the spinal operation area of swine were significantly different, and could be used as a basis for tissue recognition. In addition, SVM can effectively use the electrical impedance gap of different tissues to establish a tissue recognition method with high accuracy and good generalization, and find the critical value of impedance classification between different tissues. This study had realized 100% tissue classification by recognized electrical impedance using SVM and ensemble learning, which solved the problem of low tissue classification accuracy of current technique. In the future,

more animal experiments are needed to iteratively optimize the tissue recognition algorithm, so as to promote the application of our technique in clinical practice and provide doctors with an accurate method to recognize tissue in surgical area.

### Acknowledgements

This work was supported by the Ministry of Science and Technology, China (grant number: 2018YFB1307603) and the Natural Science Foundation of Beijing Municipality, China (grant number: L192061). There is no person who made any substantial or potential contribution to this manuscript but do not meet the criteria for authorship.

### Author Contribution

All authors had full access to the data in the study and take responsibility for the integrity of the data and the accuracy of the data analysis. Conceptualization, Y.Z., L.H., and W.Y.L.; Methodology, Y.Z., L.H.; Software, L.L. and Y.W.S.; Validation, B.R.C., J.H.L.; Investigation, B.R.C., J.H.L.; Formal Analysis, B.R.C. and Y.W.S.; Resources, Y.Z., L.H., and L.L.; Writing—Original Draft, B.R.C., Y.W.S., and J.H.L.; Writing—Review and Editing, Y.Z., L.H., J.L.Z.; Visualization, B.R.C. and Y.W.S.; Project Administration, Y.Z., L.H.; Funding Acquisition, Y.Z., L.H., W.Y.L., and J.L.Z.

B.R.C., Y.W.S., and J.H.L. should be considered joint first authors.

### Ethics Statement

The animal experiment was approved by the ethics committee of Peking Union Medical College Hospital (Ethical number: XHDW-2020-024). All authors declared that they have no conflict of interests.

### References

- Shlobin NA, Raz E, Shapiro M, Clark JR, Hoffman SC, Shaibani A, et al. Spinal neurovascular complications with anterior thoracolumbar spine surgery: a systematic review and review of thoracolumbar vascular anatomy. *Neurosurg Focus*. 2020;49(3):E9.
- Qu H, Zhao Y. Advances in tissue state recognition in spinal surgery: a review. *Front Med*. 2021;15(4):575–84.
- Khan A, Soliman MAR, Lee NJ, Waqas M, Lombardi JM, Boddapati V, et al. CT-to-fluoroscopy registration versus scan-and-plan registration for robot-assisted insertion of lumbar pedicle screws. *Neurosurg Focus*. 2022;52(1):E8.
- Pang S, Pang C, Su Z, Lin L, Zhao L, Chen Y, et al. DGMSNet: spine segmentation for MR image by a detection-guided mixed-supervised segmentation network. *Med Image Anal*. 2022;75:102261.
- Zhang J, Li W, Hu L, Yu Z, Wang T. A robotic system for spine surgery positioning and pedicle screw placement. *Int J Med Robot + Comput Assist Surg: MRCAS*. 2021;17(4):e2262.
- Qu H, Geng B, Chen B, Zhang J, Yang Y, Hu L, et al. Force perception and bone recognition of vertebral lamina milling by robot-assisted ultrasonic bone scalpel based on backpropagation neural network. *IEEE Access*. 2021;9:52101–12.
- Guan F, Sun Y, Qi X, Hu Y, Yu G, Zhang J. State recognition of bone drilling based on acoustic emission in pedicle screw operation. *Sensors (Basel, Switzerland)*. 2018;18(5):1484.
- Li Z, Chen C, Lin Y, Li X, Tan H, Chan MT, et al. A novel probe for measuring tissue bioelectrical impedance to enhance pedicle screw placement in spinal surgery. *Am J Transl Res*. 2018;10(7):2205–12.
- Park J, Choi W-M, Kim K, Jeong W-I, Seo J-B, Park I. Biopsy needle integrated with electrical impedance sensing microelectrode Array towards real-time needle guidance and tissue discrimination. *Sci Rep*. 2018;8(1):264.
- Heileman K, Daoud J, Tabrizian M. Dielectric spectroscopy as a viable biosensing tool for cell and tissue characterization and analysis. *Biosens Bioelectron*. 2013;49:348–59.
- Park J, Kim S, Park I, editors. A multi-pair electrode based impedance sensing biopsy needle for tissue discrimination during biopsy process. 2014 36th Annual International Conference of the IEEE Engineering in Medicine and Biology Society; 2014 26–30 Aug. 2014.
- Shao F, Bai H, Tang M, Xue Y, Dai Y, Zhang J. Tissue discrimination by bioelectrical impedance during PLL resection in anterior decompression surgery for treatment of cervical spondylotic myelopathy. *J Orthopaed Surg Res*. 2019;14(1):341.
- Cervantes J, Garcia-Lamont F, Rodríguez-Mazahua L, Lopez A. A comprehensive survey on support vector machine classification: applications, challenges and trends. *Neurocomputing*. 2020;408:189–215.
- Cervantes J, Lamont FG, López-Chau A, et al. Data selection based on decision tree for SVM classification on large data sets. *Appl Soft Comput*. 2015;37:787–98.
- Wang M, Chen H. Chaotic multi-swarm whale optimizer boosted support vector machine for medical diagnosis. *Appl Soft Comput*. 2020;88:105946.
- Liang X, Zhu L, Huang D-S. Multi-task ranking SVM for image cosegmentation. *Neurocomputing*. 2017;247:126–36.
- Wu SX, Wai HT, Li L, Scaglione A. A review of distributed algorithms for principal component analysis. *Proc IEEE*. 2018;106(8):1321–40.
- Reddy GT, Reddy MPK, Lakshmana K, Kaluri R, Rajput DS, Srivastava G, et al. Analysis of dimensionality reduction techniques on big data. *IEEE Access*. 2020;8:54776–88.
- Sato-Ilic M. Cluster-scaled principal component analysis. *WIREs Comput Stat*. 2021;14(3):e1572.

- 20.** Zhou J, Jiang Z, Chung FL, Wang S. Formulating ensemble learning of SVMs into a single SVM formulation by negative agreement learning. *IEEE Trans Syst Man Cybernet: Syst.* 2021;51(10):6015–28.
- 21.** Dong X, Yu Z, Cao W, Shi Y, Ma Q. A survey on ensemble learning. *Front Comp Sci.* 2020;14(2):241–58.
- 22.** Sidey-Gibbons JAM, Sidey-Gibbons CJ. Machine learning in medicine: a practical introduction. *BMC Med Res Methodol.* 2019;19(1):64.
- 23.** Sedory DM, Crawford JJ, Topp RF. The reliability of the ball-tipped probe for detecting pedicle screw tract violations prior to instrumenting the thoracic and lumbar spine. *Spine.* 2011;36(6):E447–53. Epub 2010/12/24. PubMed PMID: 21178848. <https://doi.org/10.1097/BRS.0b013e3181dbfe40>
- 24.** Bolger C, Carozzo C, Roger T, McEvoy L, Nagaria J, Vanacker G, et al. A preliminary study of reliability of impedance measurement to detect iatrogenic initial pedicle perforation (in the porcine model). *Eur Spine J.* 2006;15(3):316–20. <https://doi.org/10.1007/s00586-005-1024-1>
- 25.** Kalvøy H, Frich L, Grimnes S, Martinsen OG, Hol PK, Stubhaug A. Impedance-based tissue discrimination for needle guidance. *Physiol Meas.* 2009;30(2):129–40.
- 26.** Cheng Z, Carobbio ALC, Soggiu L, Migliorini M, Guastini L, Mora F, et al. SmartProbe: a bioimpedance sensing system for head and neck cancer tissue detection. *Physiol Meas.* 2020;41(5):054003.
- 27.** Cheng Z, Davies BL, Caldwell DG, Mattos LS. A new venous entry detection method based on electrical bio-impedance sensing. *Ann Biomed Eng.* 2018;46(10):1558–67.
- 28.** Kent B, Rossa C. Electric impedance spectroscopy feature extraction for tissue classification with electrode embedded surgical needles through a modified forward stepwise method. *Comput Biol Med.* 2021;135:104522.
- 29.** Halonen S, Kari J, Ahonen P, Kronström K, Hyttinen J. Real-time bioimpedance-based biopsy needle can identify tissue type with high spatial accuracy. *Ann Biomed Eng.* 2019;47(3):836–51.
- 30.** Halonen S, Annala K, Kari J, Jokinen S, Lumme A, Kronström K, et al. Detection of spine structures with bioimpedance probe (BIP) needle in clinical lumbar punctures. *J Clin Monit Comput.* 2017;31(5):1065–72.
- 31.** Wyss Balmer T, Ansó J, Muntane E, Gavaghan K, Weber S, Stahel A, et al. In-vivo electrical impedance measurement in mastoid bone. *Ann Biomed Eng.* 2017;45(4):1122–32.
- 32.** Esteve A, Kuprel B, Novoa RA, Ko J, Swetter SM, Blau HM, et al. Dermatologist-level classification of skin cancer with deep neural networks. *Nature.* 2017;542(7639):115–8.
- 33.** Dai Y, Xue Y, Zhang J, Li J, editors. Biologically-inspired auditory perception during robotic bone milling. 2017 IEEE International Conference on Robotics and Automation (ICRA); 2017 29 May-3 June 2017.
- 34.** Zhao F, Wang Z, Deng Q, Guo J. Study on impedance characteristics of Pig's bones. *Chin Med Equip.* 2011;26(4):5.
- 35.** Murphy EK, Mahara A, Khan S, Hyams ES, Schned AR, Pettus J, et al. Comparative study of separation between ex-vivo prostatic malignant and benign tissue using electrical impedance spectroscopy and electrical impedance tomography. *Physiol Meas.* 2017;38:1242–61.
- 36.** Dai Y, Xue Y, Zhang J. Drilling electrode for real-time measurement of electrical impedance in bone tissues. *Ann Biomed Eng.* 2014;42(3):579–88.
- 37.** Alam S, Moonsoo K, Jae-Young P, Kwon GR, editors. Performance of classification based on PCA, linear SVM, and Multi-kernel SVM. 2016 Eighth International Conference on Ubiquitous and Future Networks (ICUFN); 2016 5–8 July 2016.
- 38.** Shanzhi X, Peng W, Yonggui D. Measuring electrolyte impedance and noise simultaneously by triangular waveform voltage and principal component analysis. *Sensors.* 2016;16(4):576.
- 39.** Liu B. BioSeq-analysis: a platform for DNA, RNA and protein sequence analysis based on machine learning approaches. *Brief Bioinform.* 2019;20(4):1280–94.
- 40.** Liu B, Wang S, Long R, Chou K-C. iRSpot-EL: identify recombination spots with an ensemble learning approach. *Bioinformatics.* 2017;33(1):35–41.
- 41.** Liu B, Yang F, Chou K-C. 2L-piRNA: a two-layer ensemble classifier for identifying Piwi-interacting RNAs and their function. *Mol Ther – Nucl Acids.* 2017;7:267–77.